Video Article

Multimodal Bioluminescent and Positronic-emission Tomography/ Computational Tomography Imaging of Multiple Myeloma Bone Marrow Xenografts in NOG Mice

Gilbert Gastelum[1], Eric Y. Chang[2], David Shackleford[3], Nicholas Bernthal[3], Jeffery Kraut[1,3], Kevin Francis[4], Victoria Smutko[1], Patrick Frost[1,3]

[1]Greater Los Angeles Veteran Administration Healthcare System

[2]San Diego Veterans Administration Healthcare System

[3]University of California, Los Angeles

[4]Perkin Elmer

Correspondence to: Patrick Frost at pfrost@ucla.edu

URL: https://www.jove.com/video/58056
DOI: doi:10.3791/58056

Keywords: multiple myeloma, xenografts, bioluminescence, PET/CT, tumor microenvironment, bone marrow

Date Published: 12/13/2018

Citation: Gastelum, G., Chang, E.Y., Shackleford, D., Bernthal, N., Kraut, J., Francis, K., Smutko, V., Frost, P. Multimodal Bioluminescent and Positronic-emission Tomography/Computational Tomography Imaging of Multiple Myeloma Bone Marrow Xenografts in NOG Mice. *J. Vis. Exp.* (), e58056, doi:10.3791/58056 (2018).

Abstract

Multiple myeloma (MM) tumors engraft in the bone marrow (BM) and their survival and progression are dependent upon complex molecular and cellular interactions that exist within this microenvironment. Yet the BM microenvironment cannot be easily replicated *in vitro*, which potentially limits the physiologic relevance of many *in vitro* and *ex vivo* experimental models. These issues can be overcome by utilizing a xenograft model in which luciferase (LUC)-transfected 8226 MM cells will specifically engraft in the mouse skeleton. When these mice are given the appropriate substrate, D-luciferin, the effects of therapy on tumor growth and survival can be analyzed by measuring changes in the bioluminescent images (BLI) produced by the tumors *in vivo*. This BLI data combined with positronic-emission tomography/computational tomography (PET/CT) analysis using the metabolic marker 2-deoxy-2-(^{18}F)fluoro-D-glucose (^{18}F-FDG) is used to monitor changes in tumor metabolism over time. These imaging platforms allow for multiple noninvasive measurements within the tumor/BM microenvironment.

Video Link

The video component of this article can be found at https://www.jove.com/video/58056/

Introduction

MM is an incurable disease made up of malignant plasma B-cells that infiltrate the BM and cause bone destruction, anemia, renal impairment, and infection. MM makes up 10% - 15% of all hematological malignancies[1] and is the most frequent cancer to involve the skeleton[2]. The development of MM stems from the oncogenic transformation of long-lived plasma cells that are established in the germinal centers of lymphoid tissues before eventually homing to the BM[3]. The BM is characterized by highly heterogeneous niches; including diverse and critical cellular components, regions of low pO_2 (hypoxia), extensive vascularization, complex extracellular matrices, and cytokine and growth factor networks, all of which contribute to MM tumorgenesis[4]. Thus, the development of a disseminated MM xenograft model characterized by tumors that are strictly engrafted in the BM would be a very powerful and clinically relevant tool to study MM pathology *in vivo*[5,6]. However, numerous technical hurdles can limit the effectiveness of most xenograft models, making them costly and difficult to apply. This includes problems associated with consistent and reproducible tumor engraftment within the BM niche, a prolonged time to tumor development, and limitations in the ability to directly observe and measure changes of tumor growth/survival without having to sacrifice mice during the course of the experiment[7,8].

This protocol uses a modified xenograft model that was initially developed by Miyakawa *et al.*[9], in which an intravenous (IV) challenge with myeloma cells results in "disseminated" tumors that consistently and reproducibly engraft in the BM of NOD/SCID/IL-2γ(null) (NOG) mice[10]. The *in situ* visualization of these tumors is achieved by the stable transfection of the 8226 human MM cell line with a LUC allele and serially measuring the changes in the BLI produced by these engrafted tumor cells[6]. Importantly, this model can be expanded to utilize various other LUC-expressing human MM cell lines (*e.g.*, U266 and OPM2) with a similar propensity to specifically engraft in the skeleton of NOG mice. The identification of the tumors by bioluminescent imaging of the mice is followed by measuring the uptake of radiopharmaceutical probes (such as ^{18}F-FDG) by PET/CT. Together, this allows for additional characterization of critical biochemical pathways (*i.e.*, alterations in metabolism, changes in hypoxia, and the induction of apoptosis) within the tumor/BM microenvironment. The major strengths of this model can be highlighted by the availability of a wide range of radiolabeled, bioluminescent and fluorescent probes and markers that can be used to study MM progression and pathology *in vivo*.

Protocol

All animal procedures described below were approved by the Institutional Animal Care and Use Committee (IACUC) of the Greater Los Angeles VA Healthcare system and were performed under sterile and pathogen-free conditions.

1. Preparation of Luciferase-expressing 8226 Cells (8226-LUC)

1. Maintain the human MM cell line, 8226, in RPMI-1640 medium supplemented with 10% fetal bovine serum (FBS) and 1% penicillin-streptomycin at 37 °C in a humidified atmosphere containing 95% air and 5% carbon dioxide (CO_2).
2. Generate stable LUC-expressing reporter 8226 cells by transfecting 1 x 10^6 8226 cells with a luciferase reporter vector followed by a selection with hygromycin (100 - 350 mg/mL) as previously described[6].
3. Maintain the cells under standard sterile culturing conditions for 2 - 3 weeks, changing the medium every other day, until the establishment of a stably transfected 8226 cell line has been generated.
4. Confirm the *in vitro* luciferase activity in 1 x 10^6 transfected cells/100 µL of phosphate buffered saline (PBS) by adding the luciferase substrate, D-luciferin (150 µg/mL working solution in prewarmed culture medium), and measuring the bioluminescence of the cells in a test tube or 96-well plate using a luminometer[6].

2. Orthotopic Xenograft Model

1. Maintain NOG mice (4 - 6 weeks old, male or female) under sterile/pathogen-free conditions in an appropriate animal care facility.
2. Prepare the 8226 LUC-transfected cells for IV injection into the NOG mice (~5 x 10^6 cells/mouse) on the day of the experiment. Wash the cells 3x in ice-cold PBS, count them, and resuspend them in ice-cold PBS (minus antibiotics and FBS) at a final concentration of 5 x 10^6 cells/200 µL of PBS) in a sterile test tube. Keep the cells on ice and challenge the mice as soon as possible (within 30 - 120 min).
3. Anesthetize the mouse (with isoflurane, 1% - 3% in air at 0.5 - 1 L/min) and place the animal in a supine position on a heating pad with the head facing away. Check the level of anesthetization by pinching the toe. Apply ophthalmic ointment to the eyes.
4. Inject the 8226-LUC cells into the mice through the tail vein (200 µL/injection) using a 1 mL insulin syringe and a 26-G needle.
   Note: A heat lamp can be used to warm the tail, thereby dilating the vein and increasing the efficacy of injections.
5. Return the animal to their home cage and monitor the animals until they have fully recovered.
6. Confirm the engraftment of 8226-LUC cells in the mouse skeleton by measuring the BLI in anesthetized mice (described below and shown in **Figure 1A**).
   Note: BM exudates can also be stained for human CD45 expression using flow cytometry (**Figure 1B**) or by the immunohistochemistry of harvested bone (**Figure 1C**).

3. Measurement of BLI *In Vivo*

Note: Typically, measurable BLI from engrafted tumors in mice can be observed first between 10 - 20 days postchallenge, but this may need to be experimentally determined.

1. Anesthetize the mouse (with isoflurane, 1% - 3% in air at 0.5 - 1 L/min) and check the level of anesthetization by pinching the toe. Apply ophthalmic ointment to its eyes.
2. Give the animal an IP injection (200 µL/injection) of "*in vivo*-grade" D-luciferin substrate (30 mg/mL diluted in sterile saline).
3. Measure the BLI within 5 - 10 min, following the injection of the luciferin substrate (although the BLI activity can be observable in the mice for up to 45 - 60 min), by placing the anesthetized animal in a supine position in a small-animal imaging system (**Figure 2**). Select luminescent and X-ray analysis and acquire images (**Figure 3**).
   1. Measure the average radiance (photons/s/cm^2/steradian) in selected regions of interest (ROIs) using imaging software (**Figure 4**).
   2. Return the animal to its home cage and monitor it until it has fully recovered (approximately 15 - 20 min).

4. Treatment of the Mice with Targeted Therapy

1. Measure the baseline BLI and randomize the animals into treatment groups (4 - 8 mice/group).
2. Treat the mice with an IP injection (200 µL/injection) of temsirolimus (0.2 - 40 mg/kg mouse) using a regimen of five daily IP injections followed by 2 days of rest and an additional five daily injections[11].
3. Measure the luciferase activity (photons/s/cm^2/steradian) 2x per week as described in section 3 and plot the change of the BLI over time. Changes in tumor BLI can be presented as serial images of the mice (**Figure 5B**).
   Note: It is recommended that daily monitoring of the animals be performed until they present the following symptoms (typically within 45 - 60 days of the initial challenge): weight loss (loss of more than 10% relative to the weight prior to implantation) and/or hind limb paralysis, at which time they should be euthanized using a CO_2 chamber followed by cervical dislocation.

5. PET/CT Analysis Using ^{18}F-FDG to Measure Changes in Tumor Metabolism

1. Fast the animals in their home cage by removing their food for 24 h prior to the experiment to avoid excess non-specific uptake of ^{18}F-FDG.
2. Prepare ^{18}F-radiolabeled FDG PET probes (50 - 100 µCi/injection in sterile saline) on the day of the experiment. Record the time and activity of the ^{18}F-FDG probe with a dose calibrator.
   Note: Because ^{18}F has a relatively short half-life (~2 h), a careful preparation and planning for the use of these probes must be established.

3. Anesthetize the animal (with isoflurane, 1% - 3% in air at 0.5 - 1 L/min) and place it in a supine position on a heating pad with the head facing away. Check the level of anesthetization by pinching the toe. Apply ophthalmic ointment to its eyes.
4. Inject the probe *via* the tail vein (100 µL/injection) using a shielded 1 mL insulin syringe and a 26-G needle.
   Note: A heat lamp can be used to warm the tail, thereby dilating the vein and increasing the efficacy of injections.
5. Measure the residual radioactivity in the needle/syringe in a dose calibrator and note the activity and time.
   Note: The standardization of mouse incubation, dosage, and timing is essential to ensure data reproducibility and comparability.
6. Maintain the mice under anesthesia and at 37 °C using a heating pad during the whole period of probe uptake (~45 - 90 min).
   Note: It is important that the mice remain quiescent and at 37 °C to avoid non-specific uptake of the probe.
7. Stagger the injections of the ^{18}F-FDG probe to occur at approximately 20- to 30-min intervals to ensure similar labeling times in the mice.
   Note: Proper workflow and timing of the probe injections will result in optimal and reproducible imaging conditions.
8. Measure the ^{18}F-FDG activity in a PET/CT small-animal imaging system in selected regions of interest that correspond to the engrafted tumors (**Figure 6**).
   Note: Initially, a 10-min static PET exposure and a 2-min CT exposure are recommended, but the exact exposure times may need to be experimentally determined.
9. Return the animals to their home cages and monitor them until fully recovered. House the mice in a dedicated return room for 24 h while the probe decays to background levels.
   Note: Because of the short half-life of ^{18}F, multiple measurements using a fresh probe can be made as frequently as 2x per week.

Representative Results

In initial pilot studies, IV injections of 8226-LUC cells into NOD/SCID mice did not develop BM-engrafted MM tumors, although squamous MM tumors were easily formed (100% success rate). In contrast, IV challenges with 8226 cells into NOG mice generated (within 15 - 25 days) tumors in the skeleton (and only rarely formed tumors in non-skeletal tissue, such as the liver or spleen). Since tumors in the skeleton could not be visually confirmed by physically examining the animals, other methods had to be considered to confirm successful tumor engraftment and the location of the tumors within the BM (**Figure 1**). Similar to the reports by Miyakawa *et al.*[9], human IgG, produced by 8226 cells, could be detected in the serum of challenged NOG mice using ELISA (data not shown), although these data only confirmed engraftment and not the location or extent of the tumors. Serial imaging of multiple animals shows the distribution of BM-engrafted MM tumors (**Figure 4**). The BLI produced by these engrafted tumor cells can then be serially and non-invasively measured to assess changes in tumor growth and survival in mice treated with the mTOR inhibitor temsirolimus (**Figure 5**). Finally, PET/CT analysis for the uptake of ^{18}F-FDG in the tumors was used to demonstrate temsirolimus-mediated changes in glucose metabolism and that this correlated with changes in tumor growth (**Figure 6**). However, by stably transfecting 8226 cells with a luciferase allele, in conjunction with an optical imaging/X-ray analysis, the exact location and distribution of MM tumors in the mouse skeleton could be quickly and non-invasively determined.

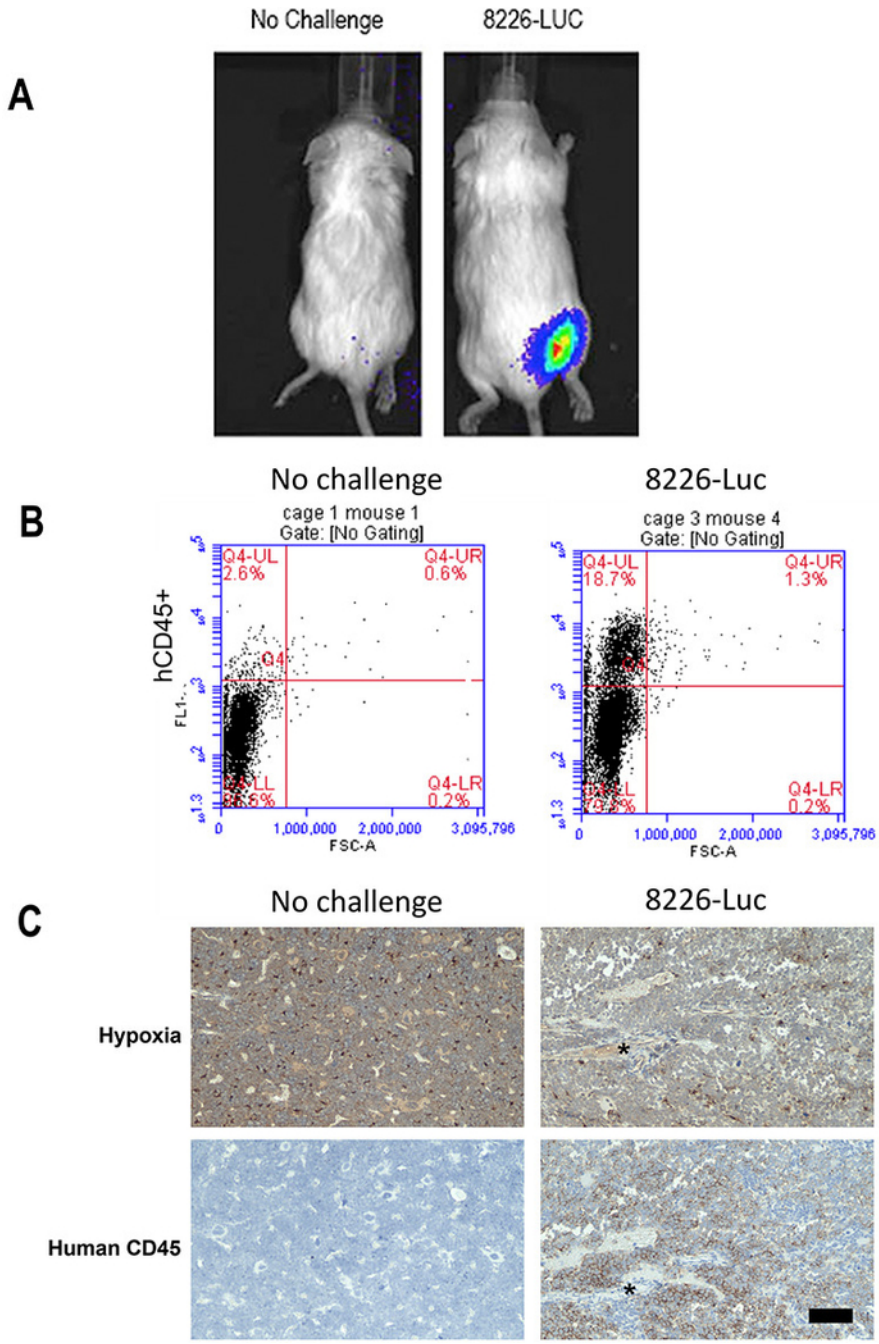

Figure 1: Confirmation of the engraftment of 8226-LUC cells in the mouse skeleton. (**A**) NOG mice were challenged with 5 x 10^6 8226-LUC2 cells IV (mouse on the left) or with saline (mouse on the right). After 15 days, the mice were given an IP injection of D-luciferin substrate and imaged using a small-animal imaging system. (**B**) The mice were sacrificed, the femurs were collected, and the BM cellular exudate was harvested. The expression of human CD45 was determined by flow cytometry using a PE-conjugated anti-human CD45 antibody. (**C**) This panel shows an immunohistochemistry of serial sections of mouse femurs stained for hypoxia using pimonidazole (top panels) or human CD45 (bottom panels) in mice challenged with 8226 (right panels) or saline (control; left panels). The asterisk indicates the location of a large blood vessel in the serial sections. The scale bar = 100 µm. Please click here to view a larger version of this figure.

Figure 2: Anesthetized NOG mice showing positioning in the imaging system prior to measuring the BLI signal from bone marrow-engrafted MM tumors. Please click here to view a larger version of this figure.

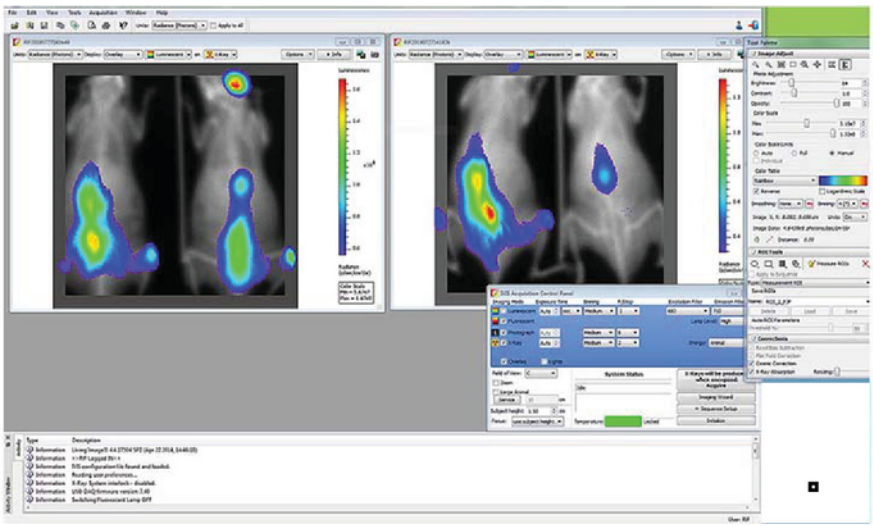

Figure 3: Set-up of the optical imaging and X-ray analysis of the bioluminescent signal collected from NOG mice. Once the animals have been successfully challenged and the engraftment of tumors in the BM has been confirmed, the mice can be randomized into treatment groups. At various times during the course of the experiment, the animals can be monitored for changes in the BLI. Because the procedure is noninvasive, the frequency of monitoring could be altered to reflect the expected growth of the tumors, as well as how quickly the cancer cells will respond to therapy. Please click here to view a larger version of this figure.

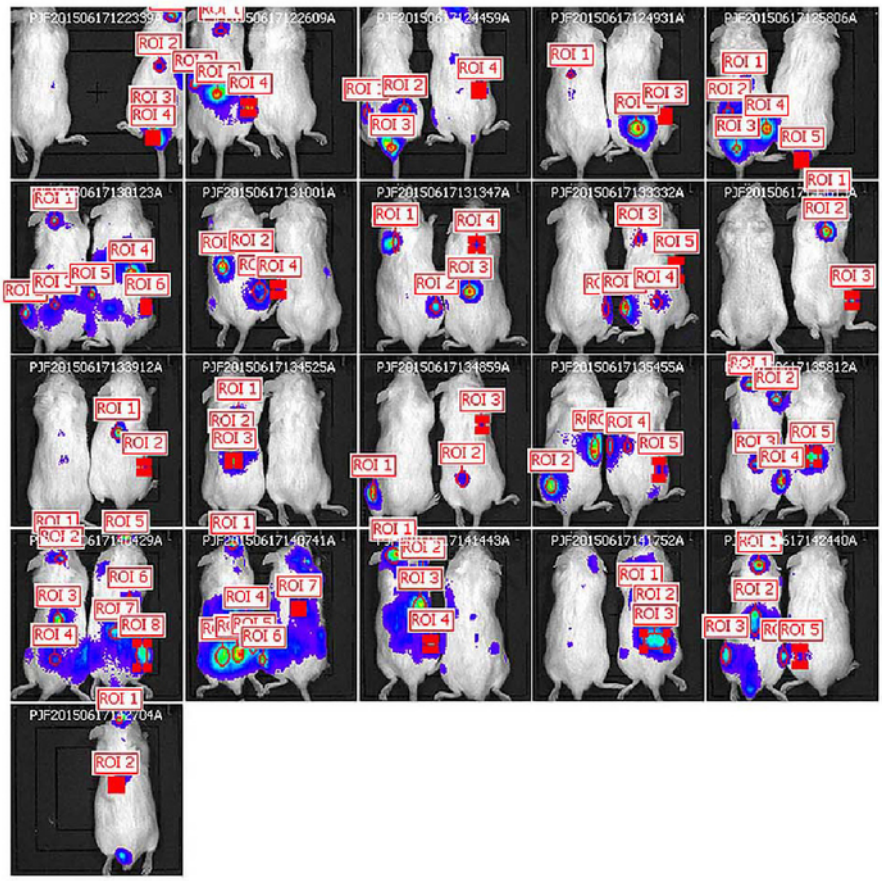

Figure 4: Serial imaging of multiple animals showing the distribution of bone marrow-engrafted MM tumors. The regions of interest (ROI) for each mouse are identified. Please click here to view a larger version of this figure.

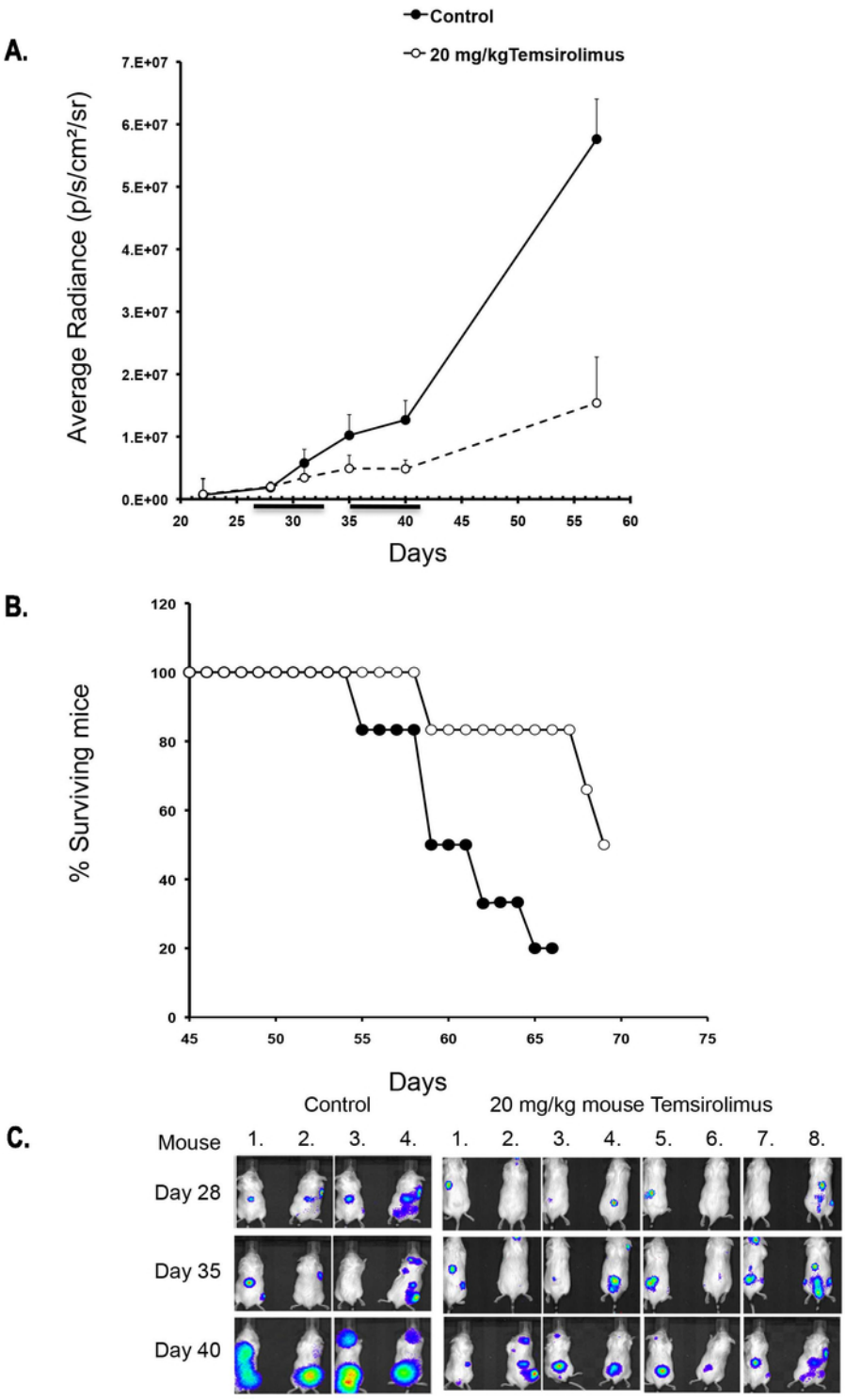

Figure 5: Changes in the BLI of engrafted tumors in NOG mice during an anti-MM therapeutic regimen. (**A**) This panel shows a change in the average radiance (p/s/cm^2/ser) in temsirolimus (20 mg/kg mouse)-treated NOG mice challenged IV with 5 x 10^6 cells. Once the mice were observed to be positive for engrafted tumors, they were randomized into various treatment groups. The mice were given five IP injections daily, followed by 2 days of rest and, then, an additional five IP injections of temsirolimus (the bars on the X-axis indicate the days of treatment) or vehicle control. On various days, the mice were given IP injections of *"in vivo*-grade" D-luciferin, and the BLI was measured using an optical imaging platform. The values represent the average radiance (p/s/cm^2/ser) ± a 95% confidence interval. (**B**) This Kaplan-Meier plot shows the change in percentage of the surviving mice over time. Mice that had reached the endpoint criteria (*i.e.*, a loss of > 10% body weight or hind-limb paralysis) were humanely euthanized. (**C**) This panel shows representative images of mice taken on days 28, 35, and 40, showing changes in the LUC activity. Please click here to view a larger version of this figure.

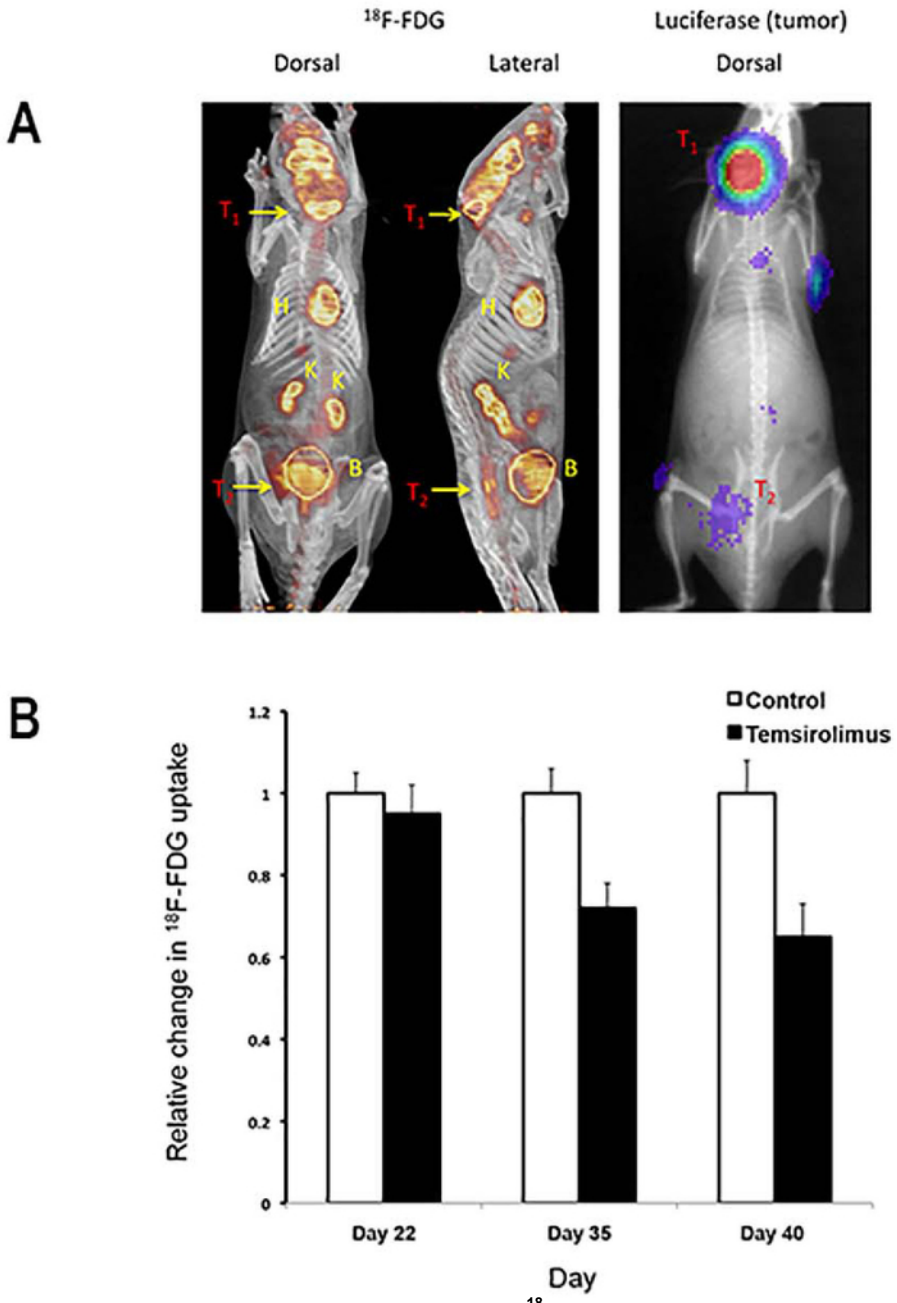

Figure 6: Serial imaging and relative changes in the ^{18}F-FDG uptake by PET/CT. (**A**) This panel shows serial imaging of the same mouse for bioluminescence (optical imaging/X-ray) imaging and ^{18}F-FDG uptake by PET/CT. BLI was measured in anesthetized mice, and the PET/CT imaging of the same mouse was performed 24 h later. The mouse fasted overnight and, on the day of the study, received an IV injection of 50 µCi ^{18}F-FDG. The mice were maintained under anesthesia during the probe uptake incubation (60 min) and, then, were analyzed for ^{18}F-FDG uptake by PET/CT analysis. Tumors (T1 and T2) are indicated.H = heart, K = kidney, and B = bladder. (**B**) This panel shows relative changes (in a percentage of untreated control tumors) in the ^{18}F-FDG uptake in control mice (no treatment) or temsirolimus (20 mg/kg mouse)-treated mice (measured at days 22, 35, and 40). The data is presented as the mean (*n* = 5 mice) ± 1 S.D. Please click here to view a larger version of this figure.

Discussion

Despite a variety of preclinical xenograft models of MM[6,9,11,12,13], the ability to study the tumor/BM interactions within the BM microenvironment remains difficult[14]. The techniques described here allow for the rapid and reproducible engraftment of 8226-LUC tumors cells in the skeleton of NOG mice.

The critical steps in this protocol involved the establishment of luciferase-expressing MM cell lines and the verification of a stable expression of luciferase *in vitro*[15]. Once the cell lines have been established, NOG mice are challenged by IV injection, and the engraftment of tumors to the skeleton is confirmed by measuring the BLI activity *in vivo* (typically within 10 - 20 days postchallenge) (**Figure 1A**). The use of NOG

mice is important because other immunodeficient strains (such as NOD/SCID) do not typically form BM-engrafted tumors. The relatively high success rate of implantation (> 90%) and the short interval to observe a positive BLI signal makes this model ideal for a high-throughput and longitudinal analysis of anti-MM therapeutic modalities (**Figure 4**). Another very important aspect of this model is that the BM-engrafted MM cell lines maintain their morphological and immunologic features of the parent cell lines (*e.g.*,8226, U266); they have consistent and reproducible growth patterns and exhibit characteristics of patient diseases, such as increasing serum human IgG paraprotein levels and the formation of bone lesions.

The advantage of this strategy is the utilization of these powerful imaging techniques to repeatedly study biochemical and molecular components of the tumor/BM microenvironment over the course of the disease progression and in response to anti-tumor therapies. In this experiment, we found that targeting mTOR activity in mice with BM-engrafted myeloma tumors resulted in a decrease in bioluminescent measurements that could be observed over time. Furthermore, we found that changes in the uptake of the ^{18}F-FDG probe (**Figure 6B**) in these same tumors were correlated to changes in the bioluminescent signal (**Figure 5B**). Another critical component of this procedure is that multiple biochemical variables can be measured within the tumor over time. This is especially important because tumor progression is a dynamic process characterized by changes in tumor physiology and microenvironment characteristics. Thus, this procedure, because of its non-invasive nature and the relatively short half-life of the probes, allows for multiple longitudinal analyses of changes in the tumor response to therapy.

After mastering the technique, the future applications of the technique present a great deal of flexibility. For example, the use of other bioluminescent or fluorescent tags (*e.g.*, fluorescently tagged antibodies) could also be utilized, as could various other ^{18}F-labeled probes and radiopharmaceutical compounds to study specific biochemical pathways or processes in the tumor/BM microenvironment. Because of the short half-life of many of these radionucleotides, multiple serial measurements could be made during the course of a specific experiment to study drug uptake, distribution, kinetics, and decay. Using this xenograft model, the ability of MM to utilize anaerobic glycolysis and other metabolic pathways (*i.e.*, fatty acid synthesis) by using other probes (*e.g.*, ^{18}F-fluoro-2deoxyglucose [^{18}F-FDG] and ^{18}F-fluoro-4-thia-palmitate [FTP])[16,17], as well as the ability to measure the anti-proliferative effects of treatment using another widely used probe (*i.e.*, 3'-deoxy-3'-[^{18}F]fluorothymidine [^{18}F-FLT]) can be included in the experimental designs. In addition, it may be possible to directly measure cell death by using ^{18}F-Annexin B1 to measure apoptosis *in vivo*[18]. Many of these compounds are commercially available.

Disclosures

The author Kevin Francis is an employee of Perkin-Elmer.

Acknowledgements

This work was supported by a VA MERIT grant1I01BX001532 from the United States Department of Veterans Affairs Biomedical Laboratory Research and Development Service (BLRDS) to P.F., and E.C. acknowledges support from the VA Clinical Science R&D Service (Merit Award I01CX001388) and VA Rehabilitation R&D Service (Merit Award I01RX002604). Further support came from a UCLA Faculty Seed Grant to J.K. These contents do not necessarily represent the views of the US Department of Veterans Affairs or the US Government.

References

1. Raab, M.S., Podar, K., Breitkreutz, I., Richardson, P.G., Anderson, K.C. Multiple Myeloma. *The Lancet*. **374** (9686), 324-339 (2009).
2. Galson, D.L., Silbermann, R., Roodman, G.D. Mechanisms of Multiple Myeloma Bone Disease. *BoneKEy Reports*. **1**, 135 (2012).
3. Anderson, K.C., Carrasco, R.D. Pathogenesis of Myeloma. *Annual Review of Pathology*. **6**, 249-274 (2011).
4. Reagan, M.R., Rosen, C.J. Navigating the Bone Marrow Niche: Translational Insights and Cancer-Driven Dysfunction. *Nature Reviews Rheumatology*. **12** (3), 154-168 (2016).
5. Frost, P. *et al.* Mammalian Target of Rapamycin Inhibitors Induce Tumor Cell Apoptosis in Vivo Primarily by Inhibiting Vegf Expression and Angiogenesis. *Journal of Oncology*. **2013**, 897025 (2013).
6. Mysore, V.S., Szablowski, J., Dervan, P.B., Frost, P.J. A DNA-Binding Molecule Targeting the Adaptive Hypoxic Response in Multiple Myeloma Has Potent Antitumor Activity. *Molecular Cancer Research*. **14** (3), 253-266 (2016).
7. Podar, K., Chauhan, D., Anderson, K.C. Bone Marrow Microenvironment and the Identification of New Targets for Myeloma Therapy. *Leukemia*. **23** (1), 10-24 (2009).
8. Campbell, R.A. *et al.* Laglambda-1: A Clinically Relevant Drug Resistant Human Multiple Myeloma Tumor Murine Model That Enables Rapid Evaluation of Treatments for Multiple Myeloma. *International Journal of Oncology*. **28** (6), 1409-1417 (2006).
9. Miyakawa, Y. *et al.* Establishment of a New Model of Human Multiple Myeloma Using Nod/Scid/Gammac(Null) (Nog) Mice. *Biochemical and Biophysical Research Communications*. **313** (2), 258-262 (2004).
10. Ito, M. *et al.* Nod/Scid/Gamma(C)(Null) Mouse: An Excellent Recipient Mouse Model for Engraftment of Human Cells. *Blood*. **100** (9), 3175-3182 (2002).
11. Frost, P. *et al.* In Vivo Antitumor Effects of the Mtor Inhibitor Cci-779 against Human Multiple Myeloma Cells in a Xenograft Model. *Blood*. **104** (13), 4181-4187 (2004).
12. Asosingh, K. *et al.* Role of the Hypoxic Bone Marrow Microenvironment in 5t2mm Murine Myeloma Tumor Progression. *Haematologica*. **90** (6), 810-817 (2005).
13. Storti, P. *et al.* Hypoxia-Inducible Factor (Hif)-1alpha Suppression in Myeloma Cells Blocks Tumoral Growth in Vivo Inhibiting Angiogenesis and Bone Destruction. *Leukemia*. **27** (8), 1697-1706 (2013).
14. Fryer, R.A. *et al.* Characterization of a Novel Mouse Model of Multiple Myeloma and Its Use in Preclinical Therapeutic Assessment. *PLoS One*. **8** (2), e57641 (2013).
15. Gould, S.J., Subramani, S. Firefly Luciferase as a Tool in Molecular and Cell Biology. *Analytical Biochemistry*. **175** (1), 5-13 (1988).
16. Czernin, J., Phelps, M.E. Positron Emission Tomography Scanning: Current and Future Applications. *Annual Review Medicine*. **53**, 89-112 (2002).

17. Pandey, M.K., Bhattacharyya, F., Belanger, A.P., Wang, S.Y., DeGrado, T.R. Pet Imaging of Fatty Acid Oxidation and Glucose Uptake in Heart and Skeletal Muscle of Rats: Effects of Cpt-1 Inhibition. *Circulation*. **122** (21) (2010).
18. Wang, M.W. *et al.* An in Vivo Molecular Imaging Probe (18)F-Annexin B1 for Apoptosis Detection by Pet/Ct: Preparation and Preliminary Evaluation. *Apoptosis*. **18** (2), 238-247 (2013).

